Fracture Mechanics of Concrete Structures, de Borst et al (eds) © 2001 Swets & Zeitlinger, Lisse, ISBN 90 2651 825 0

Interfacial debonding mechanism of FRP-strengthened concrete structures with BEM

Tian Zhi Chen & ZhiShen Wu
Department of Urban & Civil Engineering, Ibaraki University, Hitachi, Japan
Zhang Zhi Cen
Department of Engineering Mechanics, Tsinghua University, Beijing, China

ABSTRACT: In this paper, simulations of crack propagation of concrete and debonding of FRP-concrete interface in FRP-strengthened concrete structures are carried out by means of fully symmetric Galerkin multi-zone boundary element method. Cracks in concrete are considered as cohesive cracks (mode I), and the path of crack growth is priori unknown. Cracks on concrete-FRP interface are considered as cohesive shear cracks (mode II). The algorithm is given. From the numerical results, this method can deal with interfacial crack debonding and multi-crack propagation conveniently and effectively, and it is more precise than FEM. For FRP-strengthened three-point bending concrete beams, generation and propagation of diagonal crack in concrete and interfacial crack caused by diagonal crack on FRP-concrete interface is also simulated. Numerical results shows that bond quality of adhesive and stiffness of FRP sheets are very important to the strengthening effect.

1 INSTRUCTIONS

Boundary element method (BEM) is suitable for analyzing crack growth because discretization is made only on the zone boundary for elasticity, traction on the boundary can be directly calculated, and meshes are easily created (Aliabadi 1997), especially for those crack path is priori unknown. For cracks in concrete-like quasi-brittle material, the region of non-elasticity can be simplified into the cohesive crack face because the region is very narrow. Hence, non-linear fracture problem can be simplified to non-linear interface problem, and it can be solved by BEM conveniently. For example, Cen & Maier (1992) studied the cohesive crack propagation by BEM.

However, in the traditional collocation BEM, the system matrix turns out to be non-symmetric, which leads to many difficulties, e.g. it is difficult to deal with multi-crack propagation by traditional BEM. An alternative method, the Galerkin BEM (GBEM), has been proposed to formulate a symmetric system matrix in elasticity (Sirtori et al. 1992). Recently, Chen (1999) and Chen et al. (1999, submitted) proposed a fully symmetric Galerkin multi-zone boundary element method (GMZBEM), which can be used to simulate cohesive crack growth. The solving time is greatly reduced, due to the symmetry of the final system matrix. Because system equations must be solved many times during the iterative enforcement of crack propagation, advantages of GMZBEM are obvious in this field.

Fiber reinforced plastic (FRP) sheets/plates, especially carbon FRP (CFRP) sheets, are more and more widely applied in strengthened concrete structures (Wu 1997). Considerable research has been directed to investigate the application of FRP as external reinforcement primarily for strengthening the concrete structures. The loading carrying capacities and ductility can be enhanced with externally bonded FRP sheets. However, these gains may be limited by the fact that the FRP-strengthened structures can fail in several ways. Especially, debonding between FRP and concrete, which is initiated from the end of flexural cracks of concrete, is a typical failure mode.

A lot of work on this mode has been carried out theoretically, experimentally and numerically. Wu and Niu (2000) development of an analytical method on predicting the debonding failure load due to flexural cracks based on fracture energy criterion. The failure of CFRP-strengthened concrete beams (Wu et al. 1998, Yin & Wu 1999) was simulated using mixed finite element method (FEM). Yin & Wu (To appear) simulated crack propagation in FRP-strengthened concrete beams by FEM and considering cracks in concrete as smeared cracks and considering interfacial cracks between FRP and concrete as fictitious cracks. Nevertheless, for FEM, it is difficult to obtain the true tractions on crack interfaces and the stresses around the craze-tip because the meshes are complex with the growth of crack.

GMZBEM can conquer those disadvantages of FEM, and can deal with multi-crack propagation because the system matrix is symmetric. Others, in FRP-strengthened concrete structure, materials can be considered as linear-elastic and isotropic, except for cracks are treated as cohesive crack model. Cracks in concrete are mode I, and cracks on concrete-FRP interface are mode II. Multi cracks must be considered. Therefore, GMZBEM is used to simulate crack propagation of concrete and debonding of FRP-concrete interface in FRP-strengthened concrete structures in this paper. Firstly, a simple shear test, i.e. a concrete prism pasted with FRP sheets through epoxy adhesive, is considered. Secondly, propagation of five cracks in FRP-strengthened three-point bending concrete beams is calculated. To the best of the authors' knowledge, it is the first time so many cracks are simulated by means of BEM.

2 COHESIVE CRACK MODEL (CCM)

CCM is often used for quasi-brittle materials, such as rock and concrete. The cohesive crack will be formed in the direction normal to the maximum principal stress (MPS) when the MPS reaches the tensile strength σ_{max}. On the interface of the crack, a discontinuity of normal displacement Δu_n is introduced. The normal traction p_n is a decreasing function of the discontinuity. Simply, it is assumed as linear. p_n vanishes when Δu_n is larger than another material parameter w_c, and the surface where $\Delta u_n > w_c$ is called 'break'. Tangent traction on the crack face is regarded as 0 in this paper. The path of unloading is shown by an arrow in Figure 1. The area under the p_n-Δu_n curve is equal to the fracture energy G_f, and $G_f = (\sigma_{max} * w_c) / 2$.

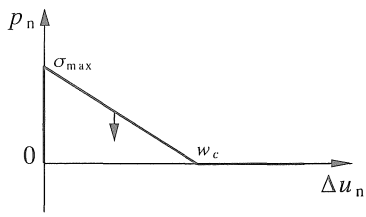

Figure 1. cohesive crack model (CCM)

Here, the traditional CCM, which is proposed for mode I, is extended to mode II, i.e. cohesive shear crack model (CSCM). According to CCM, CSCM is shown in Figure 2. τ_{max} and v_c are material parameters. Normal traction and friction on the shear crack face are omitted. The interfacial shear fracture energy is $G_{fs} = (\tau_{max} * v_c) / 2$.

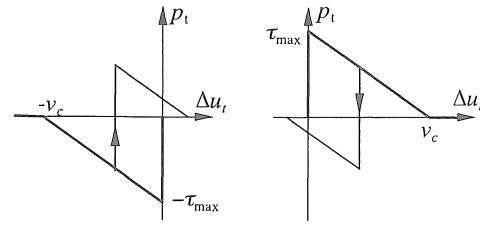

Figure 2. Cohesive shear crack model (CSCM)

3 GALERKIN MULTI-ZONE BOUNDARY ELEMENT METHOD (GMZBEM) FOR CRACK GROWTH

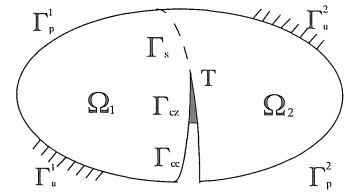

Figure 3. A two-dimensional body occupying the domain split into subdomains Ω_1 and Ω_2 by a cohesive crack interface

For the crack in Figure 3, according to reference (Chen et al. 1999, submitted), by using the same signs, the GMZBEM equation in local coordinates for subdomain i can be written as:

$$\begin{bmatrix} \tilde{A}_{uu}^{(i)} & \tilde{A}_{up}^{(i)} \\ \left[\tilde{A}_{up}^{(i)}\right]^T & \tilde{A}_{pp}^{(i)} \end{bmatrix} \begin{Bmatrix} \tilde{P}^{I(i)} \\ \tilde{U}^{I(i)} \end{Bmatrix} + \begin{bmatrix} 0 & 0 \\ \tilde{M}_{up}^{(i)} & 0 \end{bmatrix} \begin{Bmatrix} \tilde{P}^{I(i)} \\ \tilde{U}^{I(i)} \end{Bmatrix} = \begin{Bmatrix} \tilde{b}_u^{(i)} \\ \tilde{b}_p^{(i)} \end{Bmatrix} \quad (1)$$

where the system matrix is considered as the sum of a symmetric part and a non-symmetric part. the conditions for variables on interface in local coordinates are

$$\tilde{P}^{(1)} = -\tilde{P}^{(2)} = \tilde{P} \qquad \tilde{U}^{(2)} = \tilde{U}^{(1)} + \Delta\tilde{U} \quad (2a,b)$$

By adopting a proper assembly, the equation for the total structure can be obtained as

$$Ax = b + f \quad (3)$$

where

$$A = \begin{bmatrix} \tilde{A}_{uu}^{ss(1)} + \tilde{A}_{uu}^{ss(2)} & \tilde{A}_{up}^{sc(1)} & -\tilde{A}_{up}^{sc(2)} & \tilde{A}_{up}^{ss(1)} - \tilde{A}_{up}^{ss(2)} \\ \tilde{A}_{pu}^{cs(1)} & \tilde{A}_{pp}^{cc(1)} & 0 & \tilde{A}_{pp}^{cs(1)} \\ -\tilde{A}_{pu}^{cs(2)} & 0 & \tilde{A}_{pp}^{cc(2)} & \tilde{A}_{pp}^{cs(2)} \\ \left[\tilde{A}_{up}^{ss(1)} - \tilde{A}_{up}^{ss(2)}\right]^T & \tilde{A}_{pp}^{sc(1)} & \tilde{A}_{pp}^{sc(2)} & \tilde{A}_{pp}^{ss(1)} + \tilde{A}_{pp}^{ss(2)} \end{bmatrix}$$

$$x = \begin{Bmatrix} \tilde{P}^s \\ \tilde{U}^{c(1)} \\ \tilde{U}^{c(2)} \\ \tilde{U}^s \end{Bmatrix} \qquad b = \begin{Bmatrix} \tilde{b}_u^{s(1)} - \tilde{b}_u^{s(2)} \\ \tilde{b}_p^{c(1)} \\ \tilde{b}_p^{c(2)} \\ \tilde{b}_p^{s(1)} + \tilde{b}_p^{s(2)} \end{Bmatrix}$$

$$f = -\begin{bmatrix} -\tilde{A}_{up}^{ss(2)} \\ 0 \\ \tilde{A}_{pp}^{cs(2)} \\ \tilde{A}_{pp}^{ss(2)} \end{bmatrix} \{\Delta \tilde{U}^s\} - \begin{bmatrix} \tilde{A}_{uu}^{sc(1)} + \tilde{A}_{uu}^{sc(2)} \\ \left[\tilde{A}_{up}^{cc(1)}\right]^T + \tilde{M}_{up}^{cc} \\ -\left[\tilde{A}_{up}^{cc(2)}\right]^T - \tilde{M}_{up}^{cc} \\ \tilde{A}_{pu}^{sc(1)} - \tilde{A}_{pu}^{sc(2)} \end{bmatrix} \{\tilde{P}^c\}$$

Here, A is a symmetric system matrix, b represents the load and f is known on the interfaces. Obviously, the system matrix of this equation is symmetric and the non-symmetric items can only be found on the right side of the equation.

In the case of proportional loading, the load factor α is introduced as

$$b = \alpha b' \tag{4}$$

In the calculation process, to follow the quasi-static equilibrium path beyond the onset of snap through or snap-back instability, the system must be controlled by a monotone-increasing variable, which may be the load factor α, the imposed displacement or the crack length, etc.

Generally, we assume the $kk2^{th}$ degree of freedom (DOF) as the increment governing parameter (IGP) and set it as x_s in boundary element analysis. Equation 3 can be expressed as:

$$\begin{cases} Ax = \alpha b' + f \\ x_{kk2} = x_s \end{cases} \tag{5}$$

Therefore, all the unknowns on the interface can be determined by

$$\begin{cases} \alpha = \dfrac{x_s - [A^{-1}f]_{kk2}}{[A^{-1}b']_{kk2}} \\ x = \alpha A^{-1}b' + A^{-1}f \end{cases} \tag{6}$$

4 SIMULATION OF INTERFACIAL DEBONDING IN SIMPLE SHEAR TEST

To verify if GMZBEM is fit to interfacial debonding, a concrete prism pasted with CFRP sheet in Figure 4 is simulated. The cracking along the on the concrete-CFRP interface is assumed as a cohesive shear crack. The thickness b = 10 mm. CFRP parameters are: E_1 = 230,000 MPa, ν_1=0.3, and concrete parameters are: E_2 = 28,000 MPa, ν_2 = 0.15, t_2 = 60 mm. The interface crack length is set as IGP.

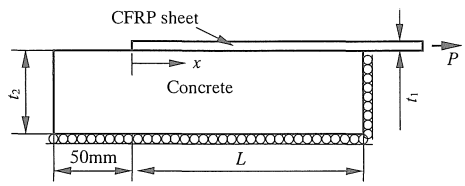

Figure 4. Structural model of simple shear specimen

In computing, the interfacial crack initiates at the load end (right end) of the FRP-concrete interface. With the crack debonding, the tangent traction on the interface moves from the right to the left like a 'wave' (Fig. 5). In the 'wave', adhesive layer transfers shear stress. Out of the 'wave', shear stress is almost zero. After the shear crack length exceeds the length of the 'wave', the load can not be increased. The wavelength is the maximum effective bond length (L_e) of the adhesive layer. Therefore, the sum of shear stress can be transferred by the FRP-concrete interface (i.e. P_{max}) is limited.

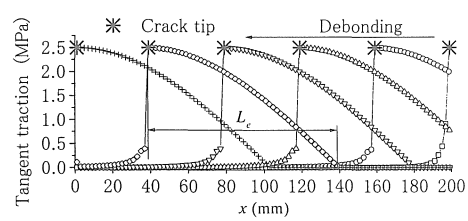

Figure 5. Tangent traction distribution on the interface (τ_{max} = 2.5 MPa, v_c = 0.48 mm, L = 200 mm)

Table 1. Material parameters and numerical results along interface

Case No.	τ_{max} (MPa)	G_{fs} (N/mm)	v_c (mm)	t_1 (mm)	L (mm)	L_e (mm)	P_{max} (N) FEM	Theory	Current study
Case 1	2.5	0.6	0.48	0.1	50	> 50	1134.8	1133.8	1135.7
Case 2	2.5	0.6	0.48	0.1	100	> 100	1562.7	1647.5	1647.3
Case 3	2.5	0.6	0.48	0.1	150	102	1562.7	1650.1	1650.7
Case 4	2.5	0.6	0.48	0.1	200	102	1562.7	1650.1	1650.7
Case 5	4.0	0.6	0.30	0.1	200	62	1589.0	1650.1	1651.3
Case 6	6.0	0.6	0.20	0.1	200	42	1593.3	1650.1	1652.4
Case 7	4.0	0.3	0.15	0.1	200	44	1123.4	1166.8	1168.6
Case 8	2.5	0.6	0.48	0.2	200	142	--	2317.9	2318.5

Table 1 shows that the numerical results in this paper agree well with the theoretical results (Yuan et al. 2001), and is more accurate than FEM results (Yin & Wu 1999). The theoretical formulation is:

$$P_{\max} = \begin{cases} \dfrac{\tau_{\max} b}{\lambda} \sin(\lambda L) & (0 \le L < \dfrac{\pi}{2\lambda}) \\ \dfrac{\tau_{\max} b}{\lambda} & (L \ge \dfrac{\pi}{2\lambda}) \end{cases} \tag{7}$$

where

$$\lambda^2 = \frac{\tau_{\max}^2}{2G_{fs}} \left(\frac{1}{E_1 t_1} + \frac{1}{E_2 t_2} \right) \tag{8}$$

From the results of Case1-4, the bond length L can influence $P_{\max}$ only if it is less than the maximum effective bond length L_e. From Case 4-7, $P_{\max}$ is independent on bond strength $\tau_{\max}$, but dependent on the value of interfacial fracture energy G_{fs}. With the same G_{fs}, $P_{\max}$ is same, even through $\tau_{\max}$ and v_c are different. With the different G_{fs}, $P_{\max}$ is also different, even through $\tau_{\max}$ is same. L_e is affected by both $\tau_{\max}$ and G_{fs}. From case 3 and 8, by using more FRP sheets, the sum of shear stress can be transferred by the interface can be increased. All of these are consistent with the theoretical results.

5 SIMULATION OF MULTI-CRACK PROPAGATION IN FRP-STRENGTHENED CONCRETE BEAMS

5.1 *Numerical model*

To strengthen the cracked concrete beam subjected to bending, FRP sheets are bonded on its tension surface by epoxy adhesive. Figure 6 shows a three-point bending concrete beam bonded with a layer of CFRP sheet, in which h denotes the length of the initial crack.

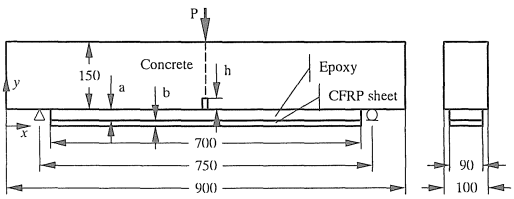

Figure 6. A CFRP-strengthened three-point bending concrete beam (unit: mm)

Experimental results showed that there are five kinds of failure modes, which are: (a) crack propagation in concrete near FRP; (b) interfacial debonding on FRP-concrete interface; (c) the propagation of flexural crack in the middle of the concrete beam; (d) the propagation of diagonal crack around the midspan; (e) the rupture of FRP. The failure mode (a) and (b) can be summed up to the growth of interfacial crack between epoxy and concrete by means of cohesive shear crack models. Thus, three kinds of cracks are considered in the numerical simulation, which are: (i) interfacial cracks between adhesive and concrete, which are mode II; (ii) flexural crack in the middle of the concrete beam, which is model I; (iii) diagonal crack around the midspan, whose growth path is priori unknown.

Because of the symmetry of the structure and the load, only a half of structure is calculated with symmetric boundary restriction on the symmetric face.

The FRP-strengthened concrete beam consists of three layers, which are concrete, epoxy and FRP. Because the epoxy and the FRP sheet are very thin, it is difficult to mesh structure in BEM. Therefore, the epoxy and the FRP sheet are considered as one layer, called strengthening layer. The thickness is the sum of the two layers and the equivalent material parameters, such as Young's modulus, are determined by the same tension deformation subjected to tension on the two ends as these two layers are considered separately.

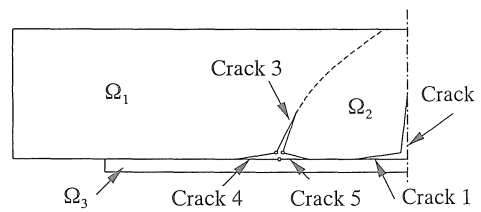

Figure 7. Numerical model

Diagonal cracks will occur as the MPS reaches the critical value in concrete near the interface. After the diagonal crack appears, the computing model should be changed from two subdomains to three subdomains (Fig. 7). Therefore, five cracks are considered.

5.2 *Algorithm*

For the propagation of one crack, the whole static evolution of crack growth can be got using the crack length as IGP. However, for the simulation of crack propagation in FRP-strengthened concrete beam, the loading point displacement (LPD) is used as IGP, because five cracks are considered and it is unknown that which one grows most easily on priori. Moreover, from the illustrations for three-point bending beam by Cen & Maier (1992), it is forecasted that LPD is a monotone-increasing variable while cracks grow with the scales in this paper.

On the other hand, the diagonal crack length should be considered as IGP in order to simulate the

propagation of the diagonal crack, especially for the crack direction. Therefore, a scheme including the above two aspects is adopted in this paper.

Based on the above scheme and GMZBEM, the simulation of multi-crack growth in FRP-strengthened concrete beam can be processed as following. ε is the demanded tolerance.

1) Estimate the path of the crack propagation, divide the region into subdomains along the path, and create boundary element mesh.

2) Form GBEM equation for each subdomain, eliminate it to the interfaces, and convert it to local interface coordinates.

3) In iteration step i, assemble the global equation, whose system matrix is symmetric, according to the proper assembly.

4) Set IGP as a certain value. Set LPD if LPD is regarded as IGP. Set the traction on the craze-tip element as $\sigma_{\max}$ if the diagonal crack length is considered as IGP.

5) Obtain the load factor and other interface unknowns by solving the equation.

6) Modify the interface conditions of the flexural crack and interface cracks by means of CCM and CSCM respectively. If the diagonal crack exists, deal with it by CCM.

7) Do the termination test of the interface condition. For mode I, if

$$\frac{\max\left|p_n^{(i)} - p_n^{(i-1)}\right|}{\sigma_{\max}} < \varepsilon \tag{9}$$

$$\frac{\max\left|\Delta u_n^{(i)} - \Delta u_n^{(i-1)}\right|}{w_c} < \varepsilon \tag{10}$$

for mode II, if

$$\frac{\max\left|p_t^{(i)} - p_t^{(i-1)}\right|}{\tau_{\max}} < \varepsilon \tag{11}$$

$$\frac{\max\left|\Delta u_t^{(i)} - \Delta u_t^{(i-1)}\right|}{v_c} < \varepsilon \tag{12}$$

go on the next step 8) because the interface condition has converged. Otherwise, go back to step 3).

8) Judge whether the diagonal crack occurs. If there is the diagonal crack, add the interface of diagonal crack, create new meshes, and then go back to step 2. Otherwise, go to step 11).

9) Compute the angle β between MPS and the out normal of the craze-tip element if the diagonal crack exists.

10) Do the termination test of the crack path. If

$$|\beta| < \varepsilon \tag{13}$$

go on the below steps because the direction of the crack has converged. Otherwise, modify the interfaces, adjust the meshes, and then go back to step 2).

11) Judge whether the diagonal crack propagates. If the diagonal crack grows by one or more elements, change IGP to the length of that crack, drive it just by one element, and go back to step 3). Otherwise, do the next step.

12) Increase LPD and go back to step 3) unless that displacement reaches the demanded value or the structure is totally destroyed.

5.3 *Numerical results*

According to the above procedures, analyses on CFRP-strengthened three-point bending concrete beams and on the strengthening effect of different factors are carried out.

Here is a typical illustration. In this example, the length of the initial crack is 25 mm. Material parameters of the concrete are: E_2 = 32500 MPa, ν_2 = 0.16, $\sigma_{\max}$ = 2.715 MPa, and w_c = 0.1105 mm. On the concrete-FRP interface, $\tau_{\max}$ = 0.5 MPa, v_c = 0.02 mm. The thickness of the strengthening layer is 1 mm, E_1 = 51060 MPa, and ν_1 = 0.30. There are 120 elements on the interface. Fine meshes are generated around the mid-span and the place where the diagonal crack probably appears. On the cross-section in the mid-span, there are 80 elements in concrete and 2 elements in strengthening layer. On the boundary of concrete and strengthening layer respectively include 270 and 244 elements.

MPS on the interface and three maximum points are shown in Figure 8, where w is LPD. Curves around the first point are smooth and it moves slowly while cracks grow. Curves around the second point are sharp. It is located in front of the craze-tip and moves along the craze-tip. If a diagonal crack initiates at the second point, it will be unloaded soon. The third point lies in the mid-span and there has been a crack at the third point. Therefore, we assume that the diagonal crack will initiate at the first maximum point.

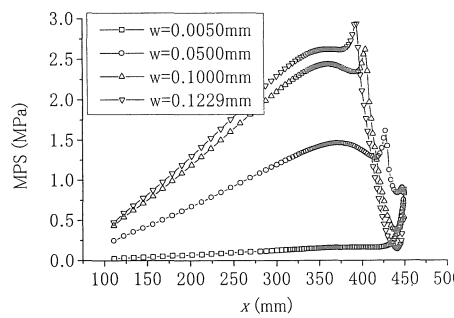

Figure 8. MPS on the interface

With the diagonal crack, 80 elements are used on the new interface. There are 197 elements and 135 interface nodes on Ω_1, 233 elements and 228 interface nodes on Ω_2, and 244 elements and 121 interface nodes on Ω_3. The interface including the diagonal crack is modified according to calculated results while cracks grow.

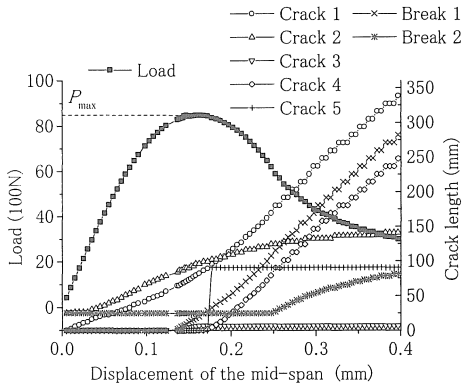

Figure 9. Relationship between the load, crack length and LPD

The relationship between the load, crack length and LPD is plotted in Figure 9, where 'break 1' and 'break 2' mean the portion totally opened and sheared, respectively. In this example, crack 1 initiates at first. After a while, crack 2 starts propagation. As the load increases, crack 3 initiates at the point 90.5mm to the mid-span. At the same time, a high shear stress concentration is induced (Fig. 10) and Crack 4 occurs after crack 3 grows by 11 elements. Then, crack 1 and crack 4 link up, and crack 3 starts unloading and stops growth. Afterwards, crack 1 and crack 2 continue propagation until rupture.

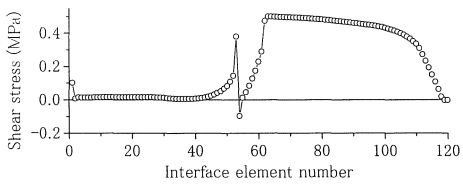

Figure 10. Shear stress on FRP-concrete interface after diagonal crack propagates

5.4 *Strengthening effect of CFRP*

Cracked concrete beams are pasted with CFRP in this section. The material parameters of the concrete are: E_2 = 32,500 MPa, ν_2 = 0.16, σ_{max} = 2.715 MPa, and w_c = 0.1105 mm. The thickness of the strengthening layer is 1 mm, E_1 = 51,060 MPa, ν_1 = 0.30. On the interface between the concrete and the layer, τ_{max} = 0.5 MPa and ν_c = 0.02 mm.

From numerical results, the effect of FRP is shown in Table 2. FRP obviously strengthens the concrete beam. The longer the initial crack is, the greater the effect is.

Table 2. Strengthening effect of CFRP sheet

h (mm)	P_{max} without FRP (N)	P_{max} With FRP (N)	$\frac{P_{max}\text{ With FRP}}{P_{max}\text{ without FRP}}$
25	6716.3	8495.9	1.2650
50	4421.4	6220.8	1.4070
100	1227.5	3061.2	2.4938

In FRP-strengthened concrete beams, FRP sheet supports the most part of the tension on the beam section. And, the tension strength of carbon fiber is much greater than the one of concrete. Therefore, the structural load carrying capacity increases.

From the point of displacement restriction, FRP sheet limits CMOD in concrete, and prevents the crack from propagation. However, as the tension subjecting to FRP must be transferred by the FRP-concrete interface, a high shear stress occurs at the end of the flexual crack on the interface. Therefore, shear cracks appear and grow. They relax the restriction of CMOD in concrete. The propagation of shear cracks reduces the strengthening effect of FRP sheet.

Figure 11 shows that the longer the initial crack is, the faster the interfacial crack grows, and the slower the flexual crack grows at beginning of loading. It can be explicated that more tension on the beam section is supported by carbon fibers.

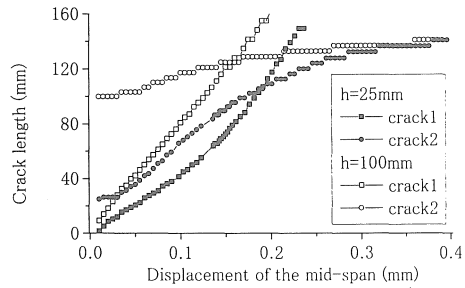

Figure 11. Crack propagate with different initial crack length

5.5 *Effect of bond quality*

To study the effect of bond quality, the same structures with h = 50 mm and ν_c = 0.02 mm for different values of τ_{max}, are modeled. Since ν_c is fixed, the

values of interfacial fracture energy G_{fs} are also different.

Table 3. Effect of bond quality

τ_{max} (MPa)	G_{fs} (N/mm)	P_{max} (N)	$\frac{P_{max}\text{ With FRP}}{P_{max}\text{ without FRP}}$
Without FRP	--	4421.4	1.0000
0.5	0.005	6220.8	1.4070
1.5	0.015	7392.1	1.6719
2.5	0.025	8313.3	1.8802
3.5	0.035	8953.3	2.0250

The results in Table 3 shows that the bond quality is very important for the strengthening effect. If the bond quality is bad, the interface cracks grow easily and the strengthening effect is bad. Otherwise, the interface cracks grow hard and the structure can bear the higher load (Fig.12). Therefore, improving the bond quality can increase the strengthening effect.

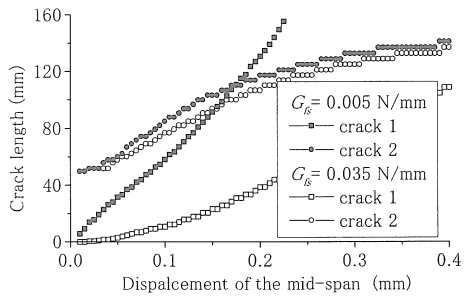

Figure 12. Crack propagate with different bond quality

Nevertheless, this enhancement is restricted by other factors, e.g. the tensile strength of FRP and the compressive strength of concrete. The structure maybe fails in abruption of carbon fibers or crush of concrete, if G_{fs} is very high. On the other hand, τ_{max} can not be too large because of failure mode (a) in Section 5.1.

5.6 *Effect of the number of strengthening layers*

Here, h = 50 mm, τ_{max} = 0.5 MPa, v_c =0.02mm. For the strengthening layer, E_1 = 230,000 MPa, ν_1=0.3, and the thickness of each layer is 0.5 mm. Structures reinforced with different number of strengthening layers are analyzed.

The different strengthening effects are shown in Table 4. Because of the added strengthening layers, the stiffness of the layers increases, so more tension subjected on carbon fibers. Then, the structure with more layers of FRP sheets can sustain higher load even if neither of these sheets ruptures.

Table 4. Effect of the number of strengthening layers

Number of layers	Thickness of strengthening layers (mm)	P_{max} (N)	$\frac{P_{max}\text{ With FRP}}{P_{max}\text{ without FRP}}$
0	0.0	4421.4	1.0000
1	0.5	5633.4	1.2741
2	1.0	6220.8	1.4070
3	1.5	6699.4	1.5152

However, the more FRP sheets are pasted, the worse marginal utility can be achieved because of interfacial debonding. The strengthening effect of the first layer is very obvious, and the effect of the second and third ones will decrease.

5.7 *Effect of CFRP sheet type*

Another way to enlarge the stiffness of strengthening layers is to increase the Young's modulus of FRP sheet. Two kinds of CFRP sheets, whose parameters are listed in Table 8, are calculated. Here, h=50mm, $\bar{\tau}$ =0.5MPa, $\bar{v}$ =0.02, and two layers of CFRP sheets are pasted in each case.

Table 5 Parameters of CFRP sheet

Model	FTS-C1-20	FTS-C6-30
Type	High strength	High modulus
Tensile strength (MPa)	3550	2500
Young's modulus (MPa)	260,000	720,000
Thickness (mm)	0.111	0.144
Thickness of each strengthening layer (mm)	0.45	0.60

The results are listed in Table 5. Because of high modulus of CFRP sheets, the strengthening effect is improved obviously.

Table 6 Effect of CFRP sheet type

Model	type	P_{max} (N)	$\frac{P_{max}\text{ With FRP}}{P_{max}\text{ without FRP}}$
Without FRP	--	4421.4	1.0000
FTS-C1-20	High strength	6353.2	1.4369
FTS-C6-30	High modulus	8235.3	1.8626

6 CONCLUSION

Based on the above numerical simulations, it can be concluded that:

1) As CCM and CSCM can simplify a FRP-strengthened concrete structure into a non-linear interface problem, and boundary conditions can be given on the interface in GMZBEM, the combination of CCM, CSCM and GMZBEM is convenient and effective to analyze the crack propagation and debonding in FRP-strengthened concrete beams.

2) GMZBEM can be used to deal with the initiation and propagation of interfacial crack debonding with softening behavior, and it is more precise than FEM. Through the numerical simulation, it is found that the load-carry capacity of interface is mainly dependent on the interfacial fracture energy and the stiffness of FRP sheets.
3) Because the system matrix of GMZBEM in this paper is fully symmetric, the time consuming on solving equations is greatly reduced. The advantages of this method are obvious in the field of crack propagation, in which system equations must be solved many times, especially for multi-crack issues. It is the first time multi-crack propagation is solved by BEM.
4) For three-point bending concrete beams. Beside the flexual crack in the center of the beam span, diagonal crack nearby the center and interfacial cracks caused by flexual crack and diagonal crack probably initiate and propagate. It shows that interfacial debonding from the end of cracks in concrete is a very important failure mode for FRP-strengthened concrete structure.
5) Bonding FRP sheets on the tensile side of concrete beam can improve the load-carry capacity of the structure. However, because of the localization of concrete cracks, it is difficult to expect large reinforcing effect due to the debonding initiating from the end of flexual crack and diagonal crack.

REFERENCE

Aliabadi, M.H. 1997. Boundary element formulations in fracture mechanics. Appl. Mech. Rev. 50(2): 83-96

Cen, Z. & Maier, G. 1992. Bifurcations and instabilities in fracture of cohesive-softening structures: a boundary element analysis. Fatigue Fract. Eng. Mater. Struct. 15(9): 911-928

Chen, T. 1999. Simulation of cohesive crack propagation & debonding by Galerkin multi-zone boundary element method. [Doctor thesis]. Beijing: Tsinghua Univ

Chen, T., Wang, B., Cen, Z. et al. 1999. A symmetric Galerkin multi-zone BEM for cohesive crack growth. Eng Frac Mech 63(5): 591-609

Chen, T., Wang, B., Cen, Z. et al. Submitted. BE analyses on multi-crack propagation & debonding in FRP strengthened concrete beam. Engineering Structure

Sirtori, S., Maier, G., Novati G. et al. 1992. A Galerkin symmetric boundary element method in elasticity: formulation and implementation. Int. J. Num. Meth. Eng. 35: 255-282

Wu, Z. 1997. Research trends on retrofitting and strengthening concrete structures by FRP sheets and plates. International Conference on Fiber Reinforced Concrete, Guangzhou, China. 9-19

Wu, Z. & Niu, H. 2000a. Study on debonding failure load of RC beams strengthened with FRP sheets. J. Struct. Eng. JSCE 46A: 1431-1441

Wu, Z. & Niu, H. 2000b. Shear transfer along FRP-concrete interface in flexural members. J materials Conc. Struct. Pavements. JSCE 49: 231-245

Wu, Z., Yin, J. & Asakura, T. 1998 Fracturing response simulation of FRP-reinforced concrete beams by mixed finite elements. J. Appl. Mech. 1:337-344

Wu, Z., Tanabe, K., Tomomasa, M. et al. 1998. A retrofitting method for concrete structures with externally prestressed carbon fiber sheets. J. Struct. Eng. JSCE 44A: 1299-1308 (in Japanese)

Yin. J. & Wu, Z. 1999. Interface crack propagation in FRP-strengthening concrete structures using nonlinear fracture mechanics. In C.W. Dolan, S.H. Rizkalla & A. Nanni (eds), Proc of the 4th Int Symp FRPRCS, Baltimore: 1035-1047. aci international

Yin, J. & Wu, Z. To appear. Simulations on crack distribution of concrete in FRP-strengthened beams with interfacial fictitious crack model. Proc. Of the 4th Int. Conf. on Fracture mechanics of concrete and concrete structures. Rotterdam: Balkema.

Yuan, H., Wu, Z. & Yoshizawa, H. 2001 Theoretical solutions on interfacial stress transfer of externally bonded steel/composite laminates. J. Struct. Mech. Earthquake Eng., JSCE 18(4)